Additional dimer-row structure of 3C-SiC(001) surfaces observed by scanning tunneling microscopy

Shiro Hara, S. Misawa, and S. Yoshida
Electrotechnical Laboratory, 1-1-4 Umezono, Tukuba-shi, Ibaraki 305, Japan

Y. Aoyagi
Riken (The Institute of Physical and Chemical Research), 2-1 Hirosawa, Wako, Saitama 351-01, Japan
(Received 4 November 1993)

We present atomic-resolution images, obtained with scanning tunneling microscopy (STM), of 3C-SiC(001) surfaces with Si adlayers on the Si-terminated surface, formed by *in situ* cleaning. We propose a unified additional dimer-row model for the surface with extra Si atoms, which is consistent with structural features obtained by our STM and low-energy-electron-diffraction (LEED) observations. The unit cell of the Si-saturated (3×2) surface seen in LEED observations consists of a pair of additional Si dimers on the Si-terminated surface. The dimer pairs form a straight string along a direction through the centers of two constituent atoms of a dimer. Unit cells of (5×2) and a new reconstruction (7×2) also consists of a pair of additional Si dimers. The (5×2) and (7×2) surfaces have $\frac{5}{3}$ and $\frac{7}{3}$ wider distances between adjacent rows than that on the (3×2), respectively. This model predicts that even number phases such as (4×2), (6×2), . . . , which are so far unobserved, are unfavorable on the excess Si surfaces in terms of structural stability. Further, it is found that the saturation of Si adsorption on the (3×2) surface is derived from a steric hindrance caused by periodic dimer-vacancy strings between the adjacent dimer pairs.

I. INTRODUCTION

The determination of crystallographic structures of reconstructed 3C-SiC(β-SiC)(001) surfaces is of both practical and fundamental importance. In terms of practical applications, the high endurance of SiC crystals in severe atmospheres, which is derived mainly from large band gaps[1] and from extreme physical and chemical hardness,[2] leads to wide applications of SiC devices to replace silicon where it is unsuitable. High-temperature,[3,4] high power,[5] radiation resistant,[6] and blue-light-emitting-diode (LED) devices[7] are examples of practical applications of SiC. In these applications, homoepitaxial layers of 3C-SiC on 3C-SiC(001) crystals heteroepitaxially grown on a Si(001) substrate are used.[8] The surface structure will provide clues about the homoepitaxial growth mechanism of 3C-SiC(001) crystals.

At a more fundamental level, SiC is one of the simplest polar surfaces of sphalerite lattice compounds to exhibit multiple reconstructions related to surface stoichiometry. Investigations of multiple reconstructions of the 3C-SiC(001) surface have been reported mainly by four groups: Dayan,[9–11] Bellina and co-workers,[12,13] Kaplan,[14,15] and our group.[16,17]

Dayan has found three surface reconstructions of (3×2), (2×1), and $c(2\times2)$, whose appearances are due to surface cleaning procedures, chiefly due to cleaning temperatures.[10] From Auger-electron spectroscopy (AES) and low-energy-electron-diffraction (LEED) analyses, he found that the amount of surface silicon (Si-to-C ratio) increases in the order of $c(2\times2)<(2\times1)<(3\times2)$. He suggested from AES analysis that these three surface phases are all Si rich.[9] Bellina and co-workers found from AES analysis that annealing in ultrahigh vacuum (UHV) over 1000 °C changes the 3C-SiC(001) surface gradually from Si rich to C rich.[12] Kaplan controlled the surface phases, namely the surface stoichiometries, by exposing to a Si molecular flux.[14] Further, our group identified the correspondence of the LEED phases to the surface elemental terminations using medium-energy ion scattering (MEIS). From the MEIS experiment, it was found that (2×1) and $c(4\times2)$ are Si terminated, and $c(2\times2)$ is C terminated, whereas (3×2) and a new phase (5×2) have an extra Si in the adlayer on the Si-terminated surface.[16] Also, the (5×2) has one less extra Si adlayer than the (3×2).[16] From an experiment on the exposure of the C-terminated $c(2\times2)$ surface at 1050 °C to Si_2H_6 gas, we found that the (3×2) surface is a Si-saturated surface, that is, no further extra Si adsorbs on this surface.[17]

In spite of these efforts, there has been little progress to determine clear surface configurations for the surfaces. In this paper, by scanning tunneling microscopy (STM) and LEED we investigate the atomic configurations of the surfaces with an extra Si adlayer: the (3×2), (5×2), and a new phase (7×2). An additional dimer row model to unify the surfaces is also proposed.

II. STRUCTURAL MODEL OF THE (3×2), (5×2), AND (7×2) RECONSTRUCTIONS

For the (3×2) surface with an extra Si adlayer, Dayan proposed a missing dimer-row model.[11] In this model the

surface is composed of extra Si dimers on the Si-terminated (2×1) surface. In the topmost layer, every third Si dimer within a dimer row is missing. The missing dimers or vacancies of dimers form straight vacancy strings perpendicular to the dimer rows, as depicted in Fig. 1(a). Here we define the direction of the dimer "row" as the [110] direction normal to the axis through the centers of the constituent two atoms within a dimer. This is a conventional way to define the dimer string direction on the Si(001) surface. In other words, the ×3 direction for 3C-SiC(001) and the ×1 direction for Si(001) are the dimer-row directions. In addition, we define a column as the normal [$\bar{1}$10] direction of the dimer-vacancy string normal to the dimer row.

If we assume that (3×2) and (5×2) structures have the same missing dimer rows, the (5×2) structure also has one missing dimer per unit cell. In other words, the (5×2) structure should have $\frac{4}{5}$ of a Si adlayer or a total Si coverage of $\Theta_{Si}=\frac{9}{5}$; that is, a larger amount of Si atoms than the $\frac{2}{3}$ of an adlayer on the (3×2) ($\Theta_{Si}=\frac{5}{3}$). This is inconsistent with the MEIS experimental result,[16] where the (5×2) structure was found to have less extra Si on the surface than the (3×2) structure.

In this paper, we propose a new (5×2) surface structural model as depicted in Fig. 1(b). This structure has $\frac{2}{5}$ of a Si adlayer ($\Theta_{Si}=\frac{7}{5}$) on the Si-terminated (2×1) surface ($\Theta_{Si}=1$). Every two adjacent Si atoms of the adlayer along the column form a dimer, which pairs with the next dimer along the row. The dimer pair, that is, four Si atoms, is the crystallographic basis of the (5×2) surface structure. The basis of the (3×2) surface structural model in Fig. 1(a) is also this dimer pair. The main difference between (3×2) and (5×2) models is the distance between the two adjacent dimer pairs in the row direction. The (3×2) surface has a dimer vacancy between the two adjacent dimer pairs, whereas the (5×2) surface has three dimer vacancies between the pairs.

Another minor difference is in the second-layer structure. At the dimer-vacancy column of the (3×2) surface, each bare Si atom with one dangling bond of each atom in the second layer forms a weak dimer with the next atom along the column to reduce the number of the dangling bonds. In the center of the dimer-vacancy columns of the (5×2) surface, Si atoms with two dangling bonds in each atom form a dimer column, which is equivalent to partial baring of the Si-terminated (2×1) surface configuration.

We apply this model to all surface structures with a Si adlayer on the (2×1) surface, like (3×2), (5×2), (7×2), and (9×2),..., that is, a [(2n +1)×2] reconstruction, where $n=1,2,3,\ldots$. The [(2n +1)×2] reconstruction has one dimer pair in the first layer and 2n −2 dimers in the second layer within a unit cell. Also, the dimers in the second layer form $n-1$ sets of Si dimer columns. The Si coverage Θ_{Si} is (2n +3)/(2n +1) monolayers (ML). The size of the unit cell is $[(2n+1)a/\sqrt{2}]\sqrt{2}a$,

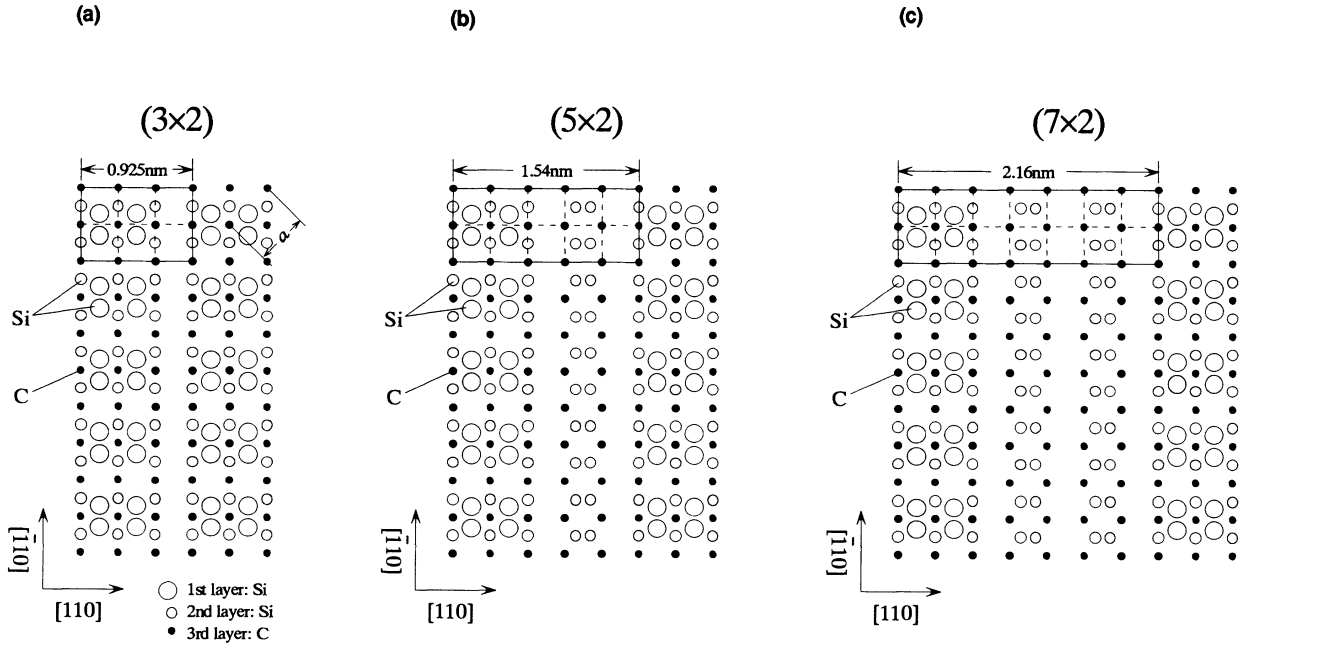

FIG. 1. (a) 3C-SiC(001)-3×2 structural model proposed by Dayan (Ref. 11). The first (close circles) and second (open circles) layers consist of Si atoms. The third layer (dotted circles) consists of C atoms. Each unit cell of the (3×2) has a Si dimer pair; that is, four Si atoms in the first layer. We refer to an atom string along the [110] direction as a row and an atom string along the [$\bar{1}$10] direction as column. This surface has a vacancy column of Si dimers every third dimer column. (b) Unified additional dimer row model of the 3C-SiC(001)-5×2 surface structure. Each unit cell of the (5×2) surface has the same Si dimer pair as the (3×2) surface. A bare area in the second layer forms one dimer column within a unit cell. (c) Unified additional dimer row model of 3C-SiC(001)-7×2 surface structure. Each unit cell of the (7×2) surface has the same Si dimer pair as the (3×2) surface. The bare area in the second layer forms two dimer columns within a unit cell.

where a is the conventional lattice constant of 3C-SiC, 0.43596 nm at 297 K.[1] For instance, the (7×2) structure for $n=3$ has four Si dimers in the second layer, which form two sets of Si dimer columns as depicted in Fig. 1(c). The dangling-bond number per unit cell is $2(2n+1)+2$, where the weak dimer in the second layer is neglected. The dangling-bond number per (1×1) area in this model converges into unity when n increases:

$$\lim_{n\to\infty}\frac{2(n+1)+2}{2(2n+1)}=1\ .$$

The surface at $n\to\infty$ is the (2×1) surface itself.

III. EXPERIMENTAL PROCEDURE

The experimental STM system used was a JEOL-4000R. The working pressure was below 7×10^{-9} Pa. An electrochemically etched tungsten tip was used. The tip was cleaned *in situ* by Si evaporation from a Si substrate at 1200 °C. This Si-capped tip generates clear Si(111)-7×7 atomic images much more easily than that without any cleaning. A 3C-SiC(001) crystal was grown on a Si(001) wafer, misoriented by $0.5°\pm0.05°$ toward [110], using chemical vapor deposition with a buffer layer technique that relaxes the lattice mismatch between the Si(001) substrate and the 3C-SiC(001) overlayer. The details of the buffer layer technique have been described elsewhere.[18] Also, such a 0.5° misoriented substrate yields a heteroepitaxial 3C-SiC layer consisting of a single domain phase.[15] The thickness of the heteroepitaxial 3C-SiC layer was about 3 μm. The heteroepitaxial layer was cut into sample pieces with a size of 1×7 mm. Before introducing the samples into the ultrahigh vacuum (UHV) chamber, each sample surface was degreased by trichloroethylene, followed by a HF rinse. In the UHV chamber it was cleaned *in situ* by raising the sample temperature up to 1150 °C for 3 min by direct current heating. From AES and LEED analyses, we had already confirmed that samples cut from the same 3C-SiC substrate form the single domain (3×2) reconstruction after the same cleaning procedure. The sample temperatures were measured by an infrared optical pyrometer whose detector wavelength was 2 μm. The emissivity of the 3C-SiC(001) through a usual 70ϕ glass view port used was 0.34.

IV. STM IMAGES OF (3×2) AND (5×2)

We observed STM atomic images of the (3×2) reconstruction for the clean surface as shown in Fig. 2. Both images (a) and (b) in the figure were atomic topographies taken in the constant current mode. The tunneling current was 0.3 nA. The sample biases were (a) -4.28 V and (b) -3.96 V. The scanning areas were (a) 50×50 nm and (b) 23×23 nm.

In Fig. 2(a), several terraces are observed. Each terrace consists of straight strings along the $[\bar{1}10]$ direction. No string along [110] is observed at any location on the sample. In general, a surface reconstruction rotates by 90° between the adjacent two terraces on the (001) surface of a tetrahedral semiconductor, when the surface has steps with a single atomic layer height. On the 3C-SiC(001) surface, from the reconstruction ordering toward the single direction and from the lack of experimental evidence of step bunching, steps are expected to have a double atomic layer height (0.22 nm).

Since the misoriented direction of the substrate is [110], the direction of the strings on each terrace is perpendicular to that direction. This is consistent with LEED analysis. From the atomic image you can see two kinds of width between adjacent strings: wide (1.5 nm) and narrow (0.9 nm). Since the length of the primitive unit cell a of the 3C-SiC(001) surface is 0.308 nm, the wide and narrow widths are $5a$ and $3a$. On terraces A, C, and D, $3a$ is dominant, whereas on terrace B, $5a$ is dominant.

Figure 2(b) is a high-resolution atomic image of terrace D. Each string along the $[\bar{1}10]$ direction consists of

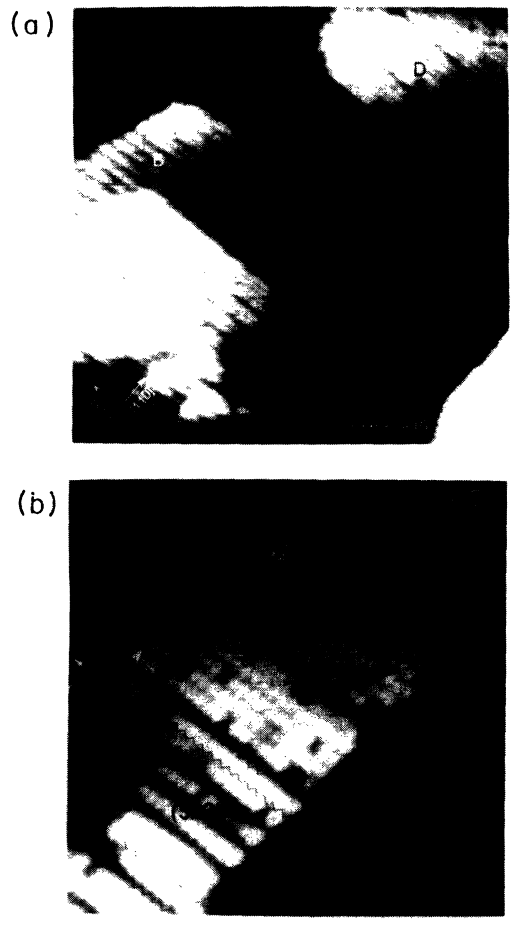

FIG. 2. Atomic-resolution images of a 3C-SiC(001)-$3\times2/5\times2$ surface measured by STM. (a) An image showing a 50×50-nm area including terraces $A-E$. The image was taken with the sample at -4.280 V and 0.3-nA tunneling current. (b) An image of terrace D of (a) at higher resolution showing a 20×20-nm area. Each oval-shaped atom group corresponds to a Si dimer pair as depicted by open circles. The main area of this terrace consists of a (3×2) reconstruction. A small area of the (5×2) surface is also seen at the lower left-hand side of the terrace. Half-unit shifts of the oval-shaped atom groups are occasionally seen as depicted by zigzag lines. The image was taken with the sample at -3.96 V and 0.3-nA tunneling current.

oval-shaped groups of Si atoms. The width of the adjacent oval-shaped atom groups along the column [$\bar{1}10$] is around 0.6 nm, which corresponds to $2a$. Since almost all widths along the row [110] are $3a$, this terrace basically consists of the (3×2) reconstruction, where each unit cell of the (3×2) reconstruction corresponds to each oval-shaped atom group. The small part of terrace D at the lower left-hand side consists of (5×2). The other part is the (3×2) area partitioned by a few $5a$ vacancy strings. You can see half-unit shifts of the unit cell or a ×1 shifts occasionally, as depicted by zigzag lines. Gaze at the figure slantwise from the lower left-hand side for an easier finding of the half-unit shifts. The shift tends to appear near edges of the (3×2) areas; that is, in the vicinity of the $5a$ vacancy strings. Most shifts extend up to the step edges of the terrace. This type of shift is also observed on terrace E. There are many missing oval-shaped atom groups, distributed randomly in the (3×2) areas. The density of the surface vacancies in these areas is around 20%, whereas in the (5×2) area few vacancies are observed.

V. DISCUSSIONS

A. Structural features of the (3×2), (5×2), and (7×2) surfaces

From the experimental results of this study and previous investigations of our group and others, several structural and chemical features of the (3×2), (5×2), and (7×2) surfaces have been found. We discuss the consistency of the features with the proposed model.

1. 90° rotation of (3×2) from (2×1)

On the Si(001)-2×1 surface, each Si atom of the first layer forms a dimer with a neighboring Si atom to reduce the dangling-bond number of the atom from 2 to 1. This is the origin of the (2×1) reconstruction. The 3C-SiC(001)-2×1 surface also has Si atoms with two dangling bonds per atom, leading to dimer formation. Conversely, on the (3×2) surface, the dimer direction in the model should rotate by 90° because the first layer has Si atoms with dangling bonds rotated 90° from that of the (2×1) surface. Actually, Kaplan has found that the direction of the ×2 reconstruction of the (3×2) surface is rotated by 90° from that of the (2×1) surface.[15] We also observed the rotation of the 2× periodicity of LEED spots when the reconstruction changed from the (2×1) to (3×2), suggesting dimer formation on the 3C-SiC(001) surfaces.

2. Hydrogenated (3×1)

We observed a phase transformation from (3×2) to (3×1) surfaces by exposing the surface to atomic hydrogen at room temperature. By raising the substrate temperature of the (3×1) surface to 1000 °C, the (3×2) surface is recovered. As far as we can observe by LEED, the conversion between (3×2) and (3×1) surfaces is reversible. The reversible process indicates that the formation of the (3×1) reconstruction needs no desorption of Si atoms. This process is evidence of hydrogen termination of the surface, in accordance with the model. The disappearance of the ×2 periodicity indicates that each surface Si atom is terminated by two hydrogen atoms to saturate the two dangling bonds. As a result, the dimers collapse. Raising the substrate temperature causes the desorption of hydrogen atoms, thus recovering the (3×2) surface. The 3× structure is kept even after prolonged hydrogenation. This suggests that the 3× structure consists of relatively large displacements of surface atoms as in a dimer vacancy, because hydrogenation generally causes no large displacement.

3. New phase (7×2)

During Si desorption caused by exposing the (3×2) surface to hydrogen at 1050 °C, we found a new phase (7×2) before the appearance of the (2×1) surface.[19] The AES peak-to-peak ratios of Si $LVV/CKLL$, normalized for the value of the (3×2) surface, are 0.87 for the (5×2) surface and 0.59 for the (7×2) surface. These values indicate that the surface Si coverages Θ_{Si} are (3×2) > (5×2) > (7×2). The normalized ratio for the Si-terminated (2×1) surface is 0.55 to 0.28. The wide range for the (2×1) surface may be due to dimer vacancies that vary the surface Si coverage. The order of the phases in terms of surface elemental compositions is consistent with our [$(2n+1)$×2] model for the Si-rich surfaces. If an intermediate composition between the (7×2) and the (2×1) surfaces is formed, we may observe a new phase (9×2) locally or throughout the surface.

4. ×1 shift of the dimer rows

On the Si(001)-2×1 surface without a vacancy string, each dimer has a relatively close correlation with the two adjacent dimers, leading to a long straight dimer row. By contrast, on the SiC(001)-3×2 surface the periodical lack of a Si dimer—that is, the independence of each dimer pair—causes the ×1 shifts of the dimer rows, as depicted by the zigzag lines in Fig. 2(b). The reasons the shifts are often seen near edges of the (3×2) terraces may be that they are preferred energetically. The shifts cause the random dispersion of the periodicity from 3× toward higher periodicities, which is reflected in the reciprocal lattice periodicity. This dispersion of the 3× periodicity is often observed experimentally as streaks instead of sharp spots in the 3× LEED pattern. Since the shift tends to occur near edges of the terraces, the fully Si-saturated (3×2) surface should exhibit sharp 3× spots instead of streaks. Actually, on the (3×2) surface after exposure to sufficient Si molecular flux or Si_2H_6 gas, we do observe sharp (3×2) spots.

5. (3×2) Si-saturated surface

From the experiment on the Si_2H_6 exposure, it has been found that the surface Si coverage Θ_{Si} saturates when the (3×2) phase forms on a substrate at a high temperature, as mentioned in Sec. I.[17] We discuss this saturation mechanism in Sec. V B.

6. A pair of dimers

In Fig. 2(b), from the measurement of the size of each oval-shaped Si-atom group, it follows that each group consists of two sets of dimers, as depicted by circles in the figure. Further, not only the (3×2) but also the (5×2) regions consist of dimer pairs. In other words, the (3×2) and (5×2) surfaces have the same crystallographic basis, in accordance with the model.

7. Comparison with GaAs(001) surfaces

Dimer vacancies are observed not only on the 3*C*-SiC(001) surface but also on the GaAs(001) surfaces, where missing dimers are general and periodical. In the As-rich GaAs(001)-*c*(4×4) surface with the As coverage $q_{As} \leq \frac{7}{4}$,[20] topmost As dimers have missing dimer columns staggered periodically every fourth column of dimers. Also, in the As-rich *c*(2×8) and (2×4) surfaces with $\Theta_{As} \leq \frac{3}{4}$,[20] surface dimers have straight missing dimer columns periodically every fourth column of dimers. The three GaAs surfaces always have one missing dimer every fourth dimer. Referring to the dimer vacancy as the "missing dimer" is reasonable on the GaAs surfaces. Conversely, on the 3*C*-SiC(001) surfaces, the number of dimer vacancies per unit cell varies widely with the Si coverage, while the number of existing Si dimers per unit cell is always 2. Crystallographically, the dimer pair is the basis. Therefore, the term "additional dimer" is better to use than "missing dimer" for the 3*C*-SiC(001) Si-rich surfaces. Pashley[21] explains the cause of missing dimers on the GaAs surfaces to be derived from a reconstruction cancelling the ionicity between III and V atoms. In the IV-IV compound, since the ionicity seems to be smaller, the mechanism for an additional dimer may be different. Actually, Pashley's electron-counting model, based on maintaining the charge neutrality,[21] is not applicable to all 3*C*-SiC(001) surfaces, (3×2) to (7×2), (2×1), and *c*(2×2). All the structural features discussed above are consistent with the unified additional dimer-row model.

B. Stability of the (3×2), (5×2), and (7×2) surfaces

1. Si saturation on (3×2)

As we have discussed previously,[17] Si epitaxy onto the (2×1) surface terminates when the (3×2) phase forms after the intermediate (7×2) and (5×2) phases. (3×2) is a final phase at a high temperature where Si desorption occurs at the same time. From an AES Si *LVV*/C *KLL* peak-to-peak ratio, the surface elemental composition was found to be constant after the (3×2) phase appears.[17] This is evidence of epitaxy saturation at the (3×2) surface. The reason for which the epitaxy terminates at the (3×2) surface with $\Theta_{Si} = \frac{5}{3}$ ML, and not at the next (2×1) with $\Theta_{Si} = 2$ ML, seems to be the difference of atomic radius between Si and C atoms. The Si diamond structure has a lattice constant larger by 20% than the 3*C*-SiC zinc-blende structure. The topmost Si atoms on the Si-terminated (2×1) surface may tend to expand by 20%, to recover the original Si-Si bond length. This leads to periodical Si vacancies on the surface. Once the (3×2) structure forms, periodical vacancy strings among dimer columns obstruct the formation of the next Si layer growth, because Si atoms can be no longer inserted there. This is a kind of steric hindrance, providing a structural explanation for the self-limiting Si growth in atomic layer epitaxy (ALE) of a 3*C*-SiC(001) crystal.[22]

2. Instability of (3×2)

In the above-mentioned ALE experiment, a slight fluctuation of the average value of the Si *LVV*/C *KLL* ratio in the (3×2) regime was observed. One possible reason for that is dimer formations by Si adatoms on the (3×2) surface. In Fig. 2(b), however, we observe no evidence of Si adatoms. Also, the adatoms increase the dangling-bond number by two per unit cell, which is energetically unfavorable. The other cause may be the random dimer vacancies observed in the STM image of Fig. 2(b).

3. Lack of observation of (4×2), (6×2), . . .

To our knowledge, no one has yet observed even number phases like (4×2),(6×2), . . . experimentally. This suggests that even phases are more unstable than odd phases. In the unified additional dimer-row model, the (5×2) or a higher odd phase has Si dimer strings in the second layer along the $[\bar{1}10]$ direction. By contrast, (4×2) or a higher even phase leaves a lone Si atom without partner Si atoms to form dimers, resulting in the unstability of even phases. This is consistent with an experimental lack of observation of even phases. When the Si coverage Θ_{Si} is $(2n+4)/(2n+2)$, corresponding to even phase $[(2n+2)\times 2]$, this phase should be split into two phases of $[(2n+1)\times 2]$ and $[(2n+3)\times 2]$. For instance, when Θ_{Si} is $\frac{6}{4}$, corresponding to the (4×2) phase, the phase splits into (5×2) and (3×2) phases. Actually, in Figs. 2(a) and 2(b), the coexistence of (5×2) and (3×2) phases are observed clearly. In other words, the surface structure we observed in the figure is the real structure of an imaginary (4×2) phase.

4. Balance between dimer vacancies and enlargement of column width

The coexistence of (3×2) and (5×2) phases is further balanced by the quantity of spot dimer vacancies. In the (3×2) areas of Fig. 2(b), the dimer vacancies are numerous, whereas in the (5×2) area at the lower left-hand side the number of vacancies is nearly zero. By forming vacancies, the Θ_{Si} of the (3×2) area approaches that of the (5×2). This causes the Si coverage on the surface to be less inhomogeneous. The additional Si coverage, without counting the second-layer Si atoms Θ_{ad} ($\Theta_{ad} = \Theta_{Si} - 1$), is about 0.54 for the actual (3×2) region,

obtained by subtracting from the ideal (3×2) coverage of 0.67 the fraction covered by vacancies (0.2×0.67). Since the actual (5×2) coverage Θ_{ad} is about 0.4, the inhomogeneity of the coverage is relatively small. If we deposit Si atoms on the surface, the area of the (5×2) surface will decrease, while that of the (3×2) will increase with small changes in the vacancy density. This is because sharp $\frac{1}{3}$ LEED spots, suggesting no vacancies, are observed only when Θ_{Si} saturates. Since the decrease in the vacancy density leads to an increase in inhomogeneity, the change of the areal fraction occupied by the (5×2) and (3×2) surfaces seems to be energetically more favorable. The vacancies vanish only after the complete disappearance of the (5×2) area by an extra Si deposition.

VI. CONCLUSION

We have observed atomic-resolution images of Si-rich 3C-SiC(001) surfaces by STM. The Si-rich (3×2), (5×2), and (7×2) surfaces are in the same reconstruction family, with additional Si dimer rows on the Si-terminated (2×1) surface. The Si coverages for these surfaces are $\frac{5}{3}$, $\frac{7}{5}$, and $\frac{9}{7}$ ML, respectively, where the topmost surface consists of a Si dimer pair per unit cell. Even number phases like (4×2), (6×2), . . ., which are so far unobserved, are unfavorable in terms of structural stability. Further, the Si epitaxy saturation or termination at the (3×2) surface is found to be due to a steric hindrance caused by periodical vacancies of dimers on the surface.

[1] *Semiconductors Group IV Elements and III-V Compounds,* edited by O. Madelung, Data in Science and Technology Vol. 1 (Springer, Berlin, 1991).

[2] *Silicon Carbide—1973,* edited by R. C. Marshall, J. W. Faust, Jr., and C. E. Ryan (University of South Carolina, Columbia, SC, 1974).

[3] Y. Kondo, T. Takahashi, K. Ishii, Y. Hayashi, E. Sakuma, S. Misawa, H. Daimon, M. Yamanaka, and S. Yoshida, Jpn. J. Appl. Phys. **26**, 310 (1987).

[4] J. W. Palmour, H. S. Kong, and R. F. Davis, J. Appl. Phys. **64**, 2168 (1988).

[5] See, for example, R. W. Keyes, *Silicon Carbide—1973* (Ref. 2), pp. 534–541.

[6] H. Itoh, N. Hayakawa, I. Nashiyama, and E. Sakuma, J. Appl. Phys. **66**, 4529 (1989).

[7] Y. Matsushita, T. Nakata, T. Uetani, T. Yamaguchi, and T. Niina, Jpn. J. Appl. Phys. **29**, L343 (1990).

[8] S. Nishino, J. A. Powell, and H. A. Will, Appl. Phys. Lett. **42**, 460 (1983).

[9] M. Dayan, Surf. Sci. **149**, L33 (1985).

[10] M. Dayan, J. Vac. Sci. Technol. A **3**, 361 (1985).

[11] M. Dayan, J. Vac. Sci. Technol. A **4**, 38 (1986).

[12] J. J. Bellina, Jr. and M. V. Zellar, Appl. Surf. Sci. **25**, 380 (1986).

[13] J. J. Bellina, Jr., J. Ferrante, and M. V. Zellar, J. Vac. Sci. Technol. A **4**, 1692 (1986).

[14] R. Kaplan, J. Vac. Sci. Technol. A **6**, 829 (1988).

[15] R. Kaplan, Surf. Sci. **215**, 111 (1989).

[16] S. Hara, W. F. J. Slijkerman, J. F. van der Veen, I. Ohdomari, S. Misawa, E. Sakuma, and S. Yoshida, Surf. Sci. **231**, L196 (1990).

[17] S. Hara, Y. Aoyagi, M. Kawai, S. Misawa, E. Sakuma, and S. Yoshida, Surf. Sci. **273**, 437 (1992).

[18] S. Yoshida, K. Sasaki, E. Sakuma, S. Misawa, and S. Gonda, Appl. Phys. Lett. **46**, 766 (1985).

[19] Such phenomena generated by hydrogen will be soon described in another paper.

[20] J. Falta, R. M. Tromp, M. Copel, G. D. Pettit, and P. D. Kirchner, Phys. Rev. Lett. **69**, 3068 (1992).

[21] M. D. Pashley, Phys. Rev. B **40**, 10 481 (1989).

[22] S. Hara, T. Meguro, Y. Aoyagi, M. Kawai, S. Misawa, E. Sakuma, and S. Yoshida, Thin Solid Films **225**, 240 (1993).

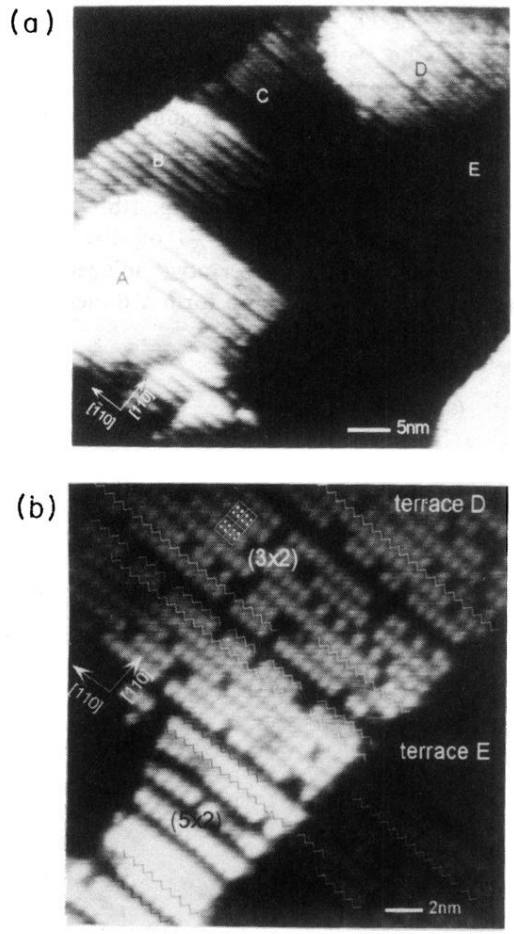

FIG. 2. Atomic-resolution images of a 3*C*-SiC(001)-3×2/5×2 surface measured by STM. (a) An image showing a 50×50-nm area including terraces *A*–*E*. The image was taken with the sample at −4.280 V and 0.3-nA tunneling current. (b) An image of terrace *D* of (a) at higher resolution showing a 20×20-nm area. Each oval-shaped atom group corresponds to a Si dimer pair as depicted by open circles. The main area of this terrace consists of a (3×2) reconstruction. A small area of the (5×2) surface is also seen at the lower left-hand side of the terrace. Half-unit shifts of the oval-shaped atom groups are occasionally seen as depicted by zigzag lines. The image was taken with the sample at −3.96 V and 0.3-nA tunneling current.